

NASA Technical Memorandum 4760  
ARL Technical Report 1389

# Rotating Shake Test and Modal Analysis of a Model Helicopter Rotor Blade

---

*W. Keats Wilkie, Paul H. Mirick, and Chester W. Langston*  
*Vehicle Technology Center*  
*U.S. Army Research Laboratory*  
*Langley Research Center • Hampton, Virginia*

Available electronically at the following URL address: <http://techreports.larc.nasa.gov/ltrs/ltrs.html>

Printed copies available from the following:

NASA Center for AeroSpace Information  
800 Elkridge Landing Road  
Linthicum Heights, MD 21090-2934  
(301) 621-0390

National Technical Information Service (NTIS)  
5285 Port Royal Road  
Springfield, VA 22161-2171  
(703) 487-4650

## Summary

Rotating blade frequencies for a model generic helicopter rotor blade mounted on an articulated hub were experimentally determined. Tests were conducted using the Aeroelastic Rotor Experimental System (ARES) tested in the Helicopter Hover Facility (HHF) at Langley Research Center. The measured data were compared with pretest analytical predictions of the rotating blade frequencies made using the MSC/NASTRAN finite-element computer code. The MSC/NASTRAN solution sequences used to analyze the model were modified to account for differential stiffening effects caused by the centrifugal force acting on the blade and rotating system dynamic effects. The correlation of the MSC/NASTRAN-derived frequencies with the experimental data is, in general, very good although discrepancies in the blade torsional frequency trends and magnitudes were observed. The procedures necessary to perform a rotating system modal analysis of a helicopter rotor blade with MSC/NASTRAN are outlined, and complete sample data deck listings are provided.

## Introduction

Calculation of the rotating system modal properties of rotor blade and hub assemblies, particularly in the case

of bearingless hub designs, often requires the use of modern finite-element computer codes. One widely used finite-element code is the commercially available MSC/NASTRAN program (refs. 1–4). Although a rotating system modal analysis can be performed using the standard release versions of MSC/NASTRAN, some potentially significant dynamic effects caused by rotation will not be accounted for properly. By modifying the standard MSC/NASTRAN solution sequence to include the additional rotational effects, a more accurate modal analysis of a rotating structure may be performed. This report documents an experimental evaluation of the ability of this modified MSC/NASTRAN procedure to accurately predict the rotating blade frequencies of a model articulated helicopter rotor blade.

## Experimental Apparatus and Procedures

### Test Facility

Tests were conducted in the Langley Helicopter Hover Facility (HHF) shown in figure 1. The HHF, a high-bay facility enclosed by a 30-ft by 30-ft by 20-ft coarse-mesh screen, is used for hover testing and rotorcraft model buildup and checkout prior to testing in the Langley Transonic Dynamics Tunnel (TDT). Models are mounted on the test stand such that the rotor plane of



Figure 1. Helicopter Hover Facility (HHF).

L-78-5962

Table 1. Properties of Model Rotor Blade

(a) Structural properties

Inboard section radius, in.	Section spar area, in <sup>2</sup>	Chordwise area moment of inertia, in <sup>4</sup>	Flapwise area moment of inertia, in <sup>4</sup>	Torsional area moment of inertia, in <sup>4</sup>	Section mass, lb/in.	Section mass moment of inertia, in-lb <sup>2</sup> /in.	Center of mass offset forward of elastic axis, in.
3.00	5.50	0.5000	0.5000	0.2632	0.4251	0.2200	0.0
6.87	0.371	0.1500	0.0500	0.1316	0.1938	0.04826	0.0
8.87	0.371	0.0250	0.0040	0.0105	0.04086	0.02505	0.0
10.625	0.371	0.0250	0.0040	0.0105	0.15113	0.05671	0.0
12.50	0.377	0.0355	0.00394	0.0394	0.14048	0.05559	0.0
13.00	0.386	0.0252	0.00249	0.00976	0.03134	0.02779	0.0
15.375	0.339	0.0252	0.00249	0.00976	0.04376	0.02961	0.0
17.85	0.278	0.03040	0.00231	0.00674	0.04123	0.02888	0.0
23.75	0.249	0.02636	0.00181	0.00565	0.0400	0.02810	0.0
28.25	0.224	0.02447	0.00151	0.00485	0.03903	0.02756	0.0
51.00	0.247	0.02447	0.00151	0.00485	0.03903	0.02756	0.0
52.75	0.279	0.02448	0.00160	0.00502	0.04125	0.02826	0.0
53.00	0.305	0.0500	0.00500	0.01435	0.07867	0.03984	-0.106
54.00	0.099	0.0400	0.00400	0.01148	0.0607	0.03563	-0.170
54.25	0.05	0.0050	0.00050	0.01435	0.01101	0.004401	-0.940

(b) Assumed material properties

Modulus of elasticity, lb/in <sup>2</sup>	Poisson's ratio
$1.0 \times 10^7$	0.3

rotation is effectively out of ground effect (15 ft, or approximately 1.6 times the rotor diameter). All hover testing in the HHF is conducted at sea level atmospheric conditions.

**Model Description**

A four-bladed articulated rotor hub, with coincident lead-lag and flapping hinges, was used in this experiment. The structural and inertial properties of the model blades are listed in table 1. The blades were rectangular in planform and possessed no built-in twist. A standard NACA 0012 airfoil contour was used over the aerodynamic portions of the blade. One blade was instrumented with flapwise, chordwise, and torsional-direction strain gauges mounted at three radial locations. The blade planform geometry, with strain-gauge locations indicated, is illustrated in figure 2.

The testbed for this experiment was the NASA/U.S. Army Aeroelastic Rotor Experimental System (ARES) model shown in figure 3. The ARES model has a streamlined fuselage shell that encloses the rotor controls and drive system. The fuselage shell, which is not usually installed when testing the ARES model in the HHF, was omitted during this test. The model rotor is powered by a variable-frequency, synchronous electric motor (rated at

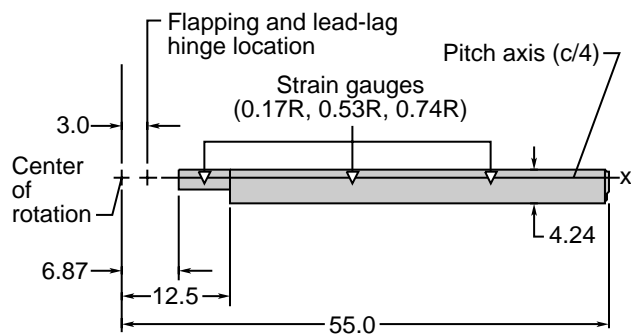


Figure 2. Rotor blade geometry.  $R$  is blade radius, and  $c$  is chord; all dimensions in inches.

47-hp output at 12000 rpm) that is connected to the rotor shaft through a belt-driven, two-stage, speed-reduction system. Collective pitch and cyclic pitch inputs are provided through a conventional swashplate arrangement. The swashplate is positioned by three electrically controlled hydraulic actuators, which are controlled remotely from the HHF control room. Signals from the blade strain gauge, as well as the signal from a strain-gauge-instrumented pitch link signal, are transferred from the rotating system to the fixed system through a 30-channel slip-ring assembly.



L-86-11,726

Figure 3. ARES model mounted in HHF.

### Test Procedure

The experimental portion of this test was designed to provide accurate measurements of elastic blade mode frequencies over a range of rotor operating speeds. The experimental procedures described below are not necessarily the ideal techniques for experimentally measuring rotating blade frequencies, but are the best use of the existing ARES hardware and instrumentation for this purpose. For this experiment, only elastic blade modes with frequencies up to and including the first torsion mode were measured. Because of the limited blade instrumentation, no attempt was made to measure blade mode shapes during this test.

Rotating-frequency measurements for each mode were made at rotor speeds that ranged from 150 rpm to 660 rpm at approximately 100-rpm intervals. The nonoscillatory collective pitch of the blades was fixed at  $0^\circ$ . At each rpm increment, the blades were excited by sinusoidally oscillating the collective pitch of the rotor with the ARES hydraulic control system. This collective pitch oscillation frequency was varied over a 10- to 20-Hz frequency band in the vicinity of each modal frequency. The amplitude of vibratory loads caused by the movement of the swashplate together with the small amount of aerodynamic excitation present from the collective pitch oscillation was sufficient to excite all of the blade modes of interest.

Blade mode frequencies were determined by processing blade and pitch-link strain-gauge signals with an

electronic signal analyzer. Output signals from the blade-mounted strain gauges were used as a measure of the blade modal deflection, while the pitch-link-mounted strain-gauge signal was used as a measure of the force input to the blade structure. From these two measurements, a frequency-response function could be generated using the signal analyzer. The frequency of the excited blade mode was then identified by looking for an amplitude peak in the frequency-response function.

Nonrotating modal frequencies were determined with a different procedure. For these measurements, the hub assembly, with a single attached blade, was removed from the ARES model and suspended so that the blade hung vertically. This method permitted measurements to be made without the blade resting on the hub flapping stops. A conventional impact-response test using a blade-mounted accelerometer, a signal analyzer, and an impact hammer was then performed. Nonrotating blade mode frequencies in this case were identified by looking for the amplitude peaks in the spectral-response function generated with the accelerometer signal.

### NASTRAN Analysis

#### Blade Analytical Model

Analysis of the articulated rotor blade was performed using several versions of the MSC/NASTRAN finite-element-analysis computer code. The original,

pretest runs were performed using MSC/NASTRAN version 66b. Subsequent runs using version 67 and, more recently, version 68 were made to verify that procedures used with previous versions were still applicable and that the results had not changed.

The blade analytical model was constructed using standard finite-element-modeling techniques. A list of the complete input data deck is provided in appendix A. All material and structural property values for the blade model were taken from values shown in table 1. The blade structure was modeled entirely with CBEAM one-dimensional beam elements, with sectional masses and mass moments of inertia for all elements modeled as nonstructural mass.

The blade-root boundary conditions were approximated by allowing rotations only about the  $Y$ - and  $Z$ -axes of the global coordinate system, which represented motion about the flapping and lead-lag hinges. The blade-root lead-lag damper was modeled using a CELAS2 scalar spring element with an appropriate damping value and a small linear spring rate. Rotation about the  $X$ -axis (blade pitching degree of freedom) was constrained to be zero, representing in essence an infinitely stiff control system.

### Rotating System Analysis Procedure

MSC/NASTRAN and COSMIC/NASTRAN have both been used to analyze the rotating modal behavior of compressor and turboprop blades (refs. 5 and 6). In these studies, plate, shell, and solid elements were used to model the blades. The computational procedure used in these studies required that two MSC/NASTRAN runs be made for each condition. First, a large-displacement analysis was made using MSC/NASTRAN solution 64. This solution sequence performs a large-displacement analysis on the rotating blade, computes steady-state displacements and stresses, and then stores the blade final stiffness and mass matrices of the blade model in a database. The frequencies and mode shapes were then computed with solution 63, using the saved matrices from the solution 64 run.

The current study also used a two-step process to obtain the blade frequencies and mode shapes although, as mentioned previously, beam elements are used here to model the rotor blade. At each desired rotor speed condition, the blade model was first analyzed using the nonlinear statics (database) MSC/NASTRAN solution sequence 66, which is the updated version of solution 64. This run calculated the deflections of the blade structure caused by a radial force field defined with the RFORCE card in the bulk data deck. Gravity forces and aerodynamic forces were neglected throughout this analysis,

and only forces acting on the blade as a result of rotation were considered. The MSC/NASTRAN executive control cards, case control cards, and bulk data used for a sample solution 66 run are included in the listing in appendix A.

Once the static analysis of the blade had been completed, a modified normal modes analysis (solution 63) was performed as a "restart" job using the MSC/NASTRAN database files generated and saved from the solution 66 run. Two modifications were made in the solution 63 DMAP code to obtain the correct rotating-blade mode shapes and frequencies of the structure. The first modification was the inclusion of a standard MSC/NASTRAN rigid format DMAP alter (RF63D89) into the solution 63 source code. This DMAP alter allowed the stiffness matrix generated and saved from the solution 66 run, which included the differential stiffening effects of the radial forces acting on the rotor blade, to be used instead of the stiffness matrix normally generated in the solution 63 run. A second DMAP modification (NLGYRO.ALT) was made to include additional centrifugal softening terms in the stiffness matrix. NLGYRO.ALT also adds Coriolis terms to the damping matrix; however, for the normal modes analysis described here, damping and Coriolis terms can be ignored. This modified solution 63 DMAP source code, with the RF63D89 and NLGYRO.ALT DMAP alters included, was then recompiled and executed as a restart job using the previously generated solution 66 database files.

The nonrotating (0-rpm) case required no initial nonlinear statics run and was performed using the unmodified solution 63 normal-modes solution sequence.

The executive control cards and case control cards necessary to execute the solution 63 runs are shown in appendix B. Changes required between MSC/NASTRAN version 68 and earlier versions (66 and 67) are noted. The RF63D89 alter code, provided in the general distribution of MSC/NASTRAN, has not been shown here. The NLGYRO.ALT alter code, which was written originally for use with version 66b and is not usually provided in the general distribution, was obtained independently from MSC. Several modifications to this DMAP alter are necessary for it to be used with MSC/NASTRAN version 68. These modifications are noted in appendix C.

### Presentation of Results

A comparison of the experimental and analytical frequency results is shown graphically in figure 4. This plot shows blade mode frequencies (Hz) versus rotor speed (rpm) for the first five elastic blade modes. The solid

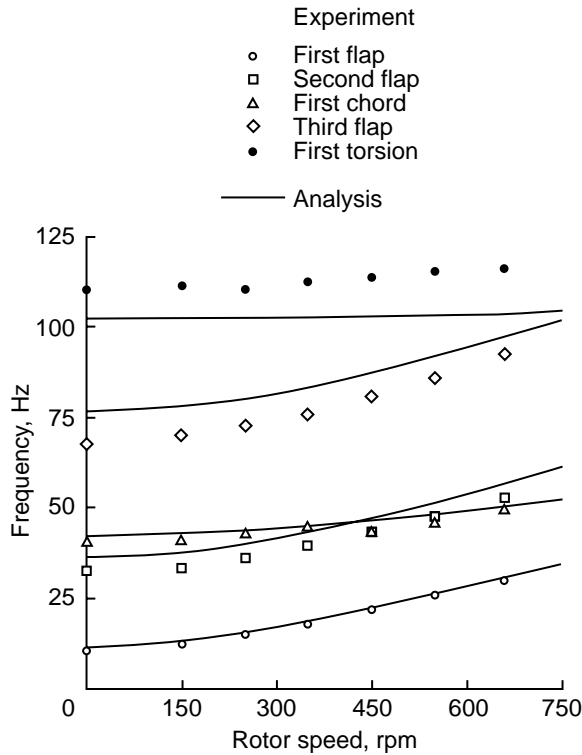


Figure 4. Comparison of experimental and analytical frequencies vs rotor speed. Rigid body flap and lead-lag modes not shown.

lines represent the analytical predictions of the blade mode frequencies made by MSC/NASTRAN. The symbols denote experimental frequency values measured in the HHF. A comparison of these experimental and analytical frequency values is also provided in table 2. Analytical calculations of the flapping and lead-lag rigid-body mode frequencies have been omitted. Repeatability in the frequency measurements was within  $\pm 1$  Hz for the three flapping modes measured, and  $\pm 2$  Hz for the chord-

wise and torsion modes. Variations in the rotor rpm settings were very small, typically less than  $\pm 2$  rpm.

### Discussion of Results

The correlation of the MSC/NASTRAN-computed, rotating-blade frequencies with the experimentally measured frequencies was, overall, very good, with the best results being obtained for the lower flapping and chord-wise modal frequencies. With the exception of blade torsion, trends in mode frequency with rotor speed were adequately predicted by the analysis. The largest discrepancies between the analytical and experimental results occurred with the third elastic flap mode results and the first torsion mode results.

The discrepancies with the third flapping mode were thought to be due to inaccurate flapping stiffness data used in defining the analytical model. MSC/NASTRAN, when given accurate structural modeling information, generally does an excellent job of predicting the non-rotating modes and frequencies of a structure. As the nonrotating-frequency calculation for this mode was still significantly in error with the experimental value, the difference is thought to be due to the structural modeling of the blade and not a fundamental error with the MSC/NASTRAN procedures used in this study.

The discrepancies in the torsional frequency magnitude are thought to be due primarily to the “infinitely stiff” control system approximation used for the blade root boundary conditions. A finite stiffness associated with the pitching degree of freedom at the root would move the frequency magnitudes upward toward the experimentally measured values. The slight upward trend of the measured frequency with rotor speed was also not predicted in the analytical results. This trend is thought to be caused by the absence of a propeller-moment-type term in the NLGYRO.ALT alter code.

Table 2. Comparison of Experimental and Analytical Blade Frequencies

Mode	Frequency, Hz at rotor speed of—													
	0 rpm		150 rpm		250 rpm		350 rpm		450 rpm		550 rpm		660 rpm	
	Exper- iment	Analysis	Exper- iment	Analysis	Exper- iment	Analysis	Exper- iment	Analysis	Exper- iment	Analysis	Exper- iment	Analysis	Exper- iment	Analysis
1st flap	10.7	11.53	12.2	13.10	14.7	15.51	17.6	18.52	21.2	21.91	24.9	25.51	28.8	29.62
2nd flap	32.6	36.38	33.1	37.64	35.8	39.78	39.0	42.77	42.7	46.44	46.7	50.63	51.75	55.69
1st chord	41.0	42.44	41.1	42.82	42.8	43.49	44.4	44.48	43.0	45.75	45.2	47.30	49.1	49.29
3rd flap	67.8	76.80	70.0	77.97	72.5	80.01	75.3	82.95	80.4	86.70	85.3	91.11	91.5	96.52
1st torsion	110.3	102.05	111.0	102.06	110.0	102.09	112.0	102.12	113.0	102.18	114.5	102.28	115.0	102.53

## **Concluding Remarks**

The rotating frequencies of a model articulated helicopter rotor blade were measured and compared to analytical frequency calculations performed using the MSC/NASTRAN finite-element structural analysis computer code. These results show that MSC/NASTRAN can, with slight modifications, adequately predict flapping and chordwise rotating modal characteristics of an

articulated helicopter rotor blade structure. Accurate prediction of torsional frequencies and trends will most likely require some additional modifications to the MSC/NASTRAN DMAP source code.

NASA Langley Research Center  
Hampton, VA 23681-0001  
January 22, 1997







GRID	1014	23.000	0.000	0.000
GRID	1015	23.750	0.000	0.000
GRID	1016	24.000	0.000	0.000
GRID	1017	25.000	0.000	0.000
GRID	1018	26.000	0.000	0.000
GRID	1019	27.000	0.000	0.000
GRID	1020	28.000	0.000	0.000
GRID	1021	28.250	0.000	0.000
GRID	1022	29.000	0.000	0.000
GRID	1023	29.150	0.000	0.000
GRID	1024	30.000	0.000	0.000
GRID	1025	31.000	0.000	0.000
GRID	1026	32.000	0.000	0.000
GRID	1027	33.000	0.000	0.000
GRID	1028	34.000	0.000	0.000
GRID	1029	35.000	0.000	0.000
GRID	1030	36.000	0.000	0.000
GRID	1031	37.000	0.000	0.000
GRID	1032	38.000	0.000	0.000
GRID	1033	39.000	0.000	0.000
GRID	1034	40.000	0.000	0.000
GRID	1035	41.000	0.000	0.000
GRID	1036	41.250	0.000	0.000
GRID	1037	42.000	0.000	0.000
GRID	1038	43.000	0.000	0.000
GRID	1039	44.000	0.000	0.000
GRID	1040	45.000	0.000	0.000
GRID	1041	46.000	0.000	0.000
GRID	1042	47.000	0.000	0.000
GRID	1043	48.000	0.000	0.000
GRID	1044	49.000	0.000	0.000
GRID	1045	50.000	0.000	0.000
GRID	1046	51.000	0.000	0.000
GRID	1047	52.750	0.000	0.000
GRID	1048	53.000	0.000	0.000
GRID	1049	54.000	0.000	0.000
GRID	1050	54.250	0.000	0.000
GRID	1051	55.000	0.000	0.000

\$

-----

\$ CONNECTIVITY:

-----

-----

\$ CBEAM    EID    PID    GA    GB    X1    X2    X3

-----2-----3-----4-----5-----6-----7-----8-----9-----A-----

CBEAM	1000	1000	1000	1001	0.0	1.0	0.0
CBEAM	1001	1001	1001	1002	0.0	1.0	0.0
CBEAM	1002	1001	1002	1003	0.0	1.0	0.0
CBEAM	1003	1001	1003	1004	0.0	1.0	0.0
CBEAM	1004	1004	1004	1005	0.0	1.0	0.0
CBEAM	1005	1004	1005	1006	0.0	1.0	0.0
CBEAM	1006	1004	1006	1007	0.0	1.0	0.0
CBEAM	1007	1004	1007	1008	0.0	1.0	0.0
CBEAM	1008	1008	1008	1009	0.0	1.0	0.0
CBEAM	1009	1008	1009	1010	0.0	1.0	0.0
CBEAM	1010	1008	1010	1011	0.0	1.0	0.0
CBEAM	1011	1008	1011	1012	0.0	1.0	0.0
CBEAM	1012	1008	1012	1013	0.0	1.0	0.0
CBEAM	1013	1008	1013	1014	0.0	1.0	0.0
CBEAM	1014	1008	1014	1015	0.0	1.0	0.0
CBEAM	1015	1015	1015	1016	0.0	1.0	0.0
CBEAM	1016	1015	1016	1017	0.0	1.0	0.0
CBEAM	1017	1015	1017	1018	0.0	1.0	0.0
CBEAM	1018	1015	1018	1019	0.0	1.0	0.0
CBEAM	1019	1015	1019	1020	0.0	1.0	0.0
CBEAM	1020	1015	1020	1021	0.0	1.0	0.0
CBEAM	1021	1021	1021	1022	0.0	1.0	0.0
CBEAM	1022	1021	1022	1023	0.0	1.0	0.0
CBEAM	1023	1021	1023	1024	0.0	1.0	0.0
CBEAM	1024	1021	1024	1025	0.0	1.0	0.0
CBEAM	1025	1021	1025	1026	0.0	1.0	0.0
CBEAM	1026	1021	1026	1027	0.0	1.0	0.0
CBEAM	1027	1021	1027	1028	0.0	1.0	0.0

CBEAM	1028	1021	1028	1029	0.0	1.0	0.0
CBEAM	1029	1021	1029	1030	0.0	1.0	0.0
CBEAM	1030	1021	1030	1031	0.0	1.0	0.0
CBEAM	1031	1021	1031	1032	0.0	1.0	0.0
CBEAM	1032	1021	1032	1033	0.0	1.0	0.0
CBEAM	1033	1021	1033	1034	0.0	1.0	0.0
CBEAM	1034	1021	1034	1035	0.0	1.0	0.0
CBEAM	1035	1021	1035	1036	0.0	1.0	0.0
CBEAM	1036	1021	1036	1037	0.0	1.0	0.0
CBEAM	1037	1021	1037	1038	0.0	1.0	0.0
CBEAM	1038	1021	1038	1039	0.0	1.0	0.0
CBEAM	1039	1021	1039	1040	0.0	1.0	0.0
CBEAM	1040	1021	1040	1041	0.0	1.0	0.0
CBEAM	1041	1021	1041	1042	0.0	1.0	0.0
CBEAM	1042	1021	1042	1043	0.0	1.0	0.0
CBEAM	1043	1021	1043	1044	0.0	1.0	0.0
CBEAM	1044	1021	1044	1045	0.0	1.0	0.0
CBEAM	1045	1021	1045	1046	0.0	1.0	0.0
CBEAM	1046	1046	1046	1047	0.0	1.0	0.0
CBEAM	1047	1047	1047	1048	0.0	1.0	0.0
CBEAM	1048	1048	1048	1049	0.0	1.0	0.0
CBEAM	1049	1049	1049	1050	0.0	1.0	0.0
CBEAM	1050	1050	1050	1051	0.0	1.0	0.0

\$

-----  
 \$ PROPERTY CARDS:  
 -----

\$

-----  
 \$ PBEAM    PID    MID    A    I1    I2    I12    J    NSM  
 -----2-----3-----4-----5-----6-----7-----8-----9-----A-----

PBEAM,1000,1000,0.377,0.03550,0.00394,,0.03940,0.14048,+P001

+P001,,,,,,,,,+P002

+P002,,,,, 5.559-2,,,,+P003

+P003, 0.00, 0.0, 0.00, 0.0

\$

PBEAM,1001,1000,0.386,0.02520,0.00249,,0.00976,0.3134-1,+P011

+P011,,,,,,,,,+P012

+P012,,,,, 2.779-2,,,,+P013

+P013, 0.00, 0.0, 0.00, 0.0

\$

PBEAM,1004,1000,0.339,0.02520,0.00249,,0.00976,0.4376-1,+P041

+P041,,,,,,,,,+P042

+P042,,,,, 2.961-2,,,,+P043

+P043, 0.00, 0.0, 0.00, 0.0

\$

PBEAM,1008,1000,0.278,0.03040,0.00231,,0.00674,0.4123-1,+P081

+P081,,,,,,,,,+P082

+P082,,,,, 2.888-2,,,,+P083

+P083, 0.00, 0.0, 0.00, 0.0

\$

PBEAM,1015,1000,0.249,0.02636,0.00181,,0.00565,0.400-1,+P151

+P151,,,,,,,,,+P152

+P152,,,,, 2.810-2,,,,+P153

+P153, 0.00, 0.0, 0.00, 0.0

\$

PBEAM,1021,1000,0.224,0.02447,0.00151,,0.00485,0.3903-1,+P211

+P211,,,,,,,,,+P212

+P212,,,,, 2.756-2,,,,+P213

+P213, 0.00, 0.0, 0.00, 0.0

\$

PBEAM,1046,1000,0.247,0.02447,0.00151,,0.00485,0.3903-1,+P461

+P461,,,,,,,,,+P462

+P462,,,,, 2.756-2,,,,+P463

+P463, 0.00, 0.0, 0.00, 0.0

\$

PBEAM,1047,1000,0.279,0.02448,0.00160,,0.00502,0.4125-1,+P471

+P471,,,,,,,,,+P472

+P472,,,,, 2.826-2,,,,+P473

+P473, 0.00, 0.0, 0.00, 0.0

\$

PBEAM,1048,1000,0.305,0.05000,0.00500,,0.01435,0.7867-1,+P481

+P481,,,,,,,,,+P482

+P482,,,,, 3.984-2,,,,+P483

```

+P483, -0.106, 0.0, -0.106, 0.0
$
PBEAM,1049,1000,0.099,0.04000,0.00400,,0.01148,0.607-1,+P491
+P491,,,,,,,,,+P492
+P492,,,,, 3.563-2,,,,,+P493
+P493, -0.17, 0.0, -0.17, 0.0
$
PBEAM,1050,1000,0.05,0.00500,0.00050,,0.01435,0.1101-1,+P501
+P501,,,,,,,,,+P502
+P502,,,,, 4.401-3,,,,,+P503
+P503, -0.940, 0.0, -0.940, 0.0
$
$-----
$ MATERIAL PROPERTY CARDS:
$-----
$ 1000: FIBERGLASS BLADE (ASSUMED PROPERTIES)
$-----
$          MID          E          G          NU          RHO
$-----2-----3-----4-----5-----6-----7-----8-----9-----A-----
MAT1      1000      1.0+7              0.3
$
$
ENDDATA

```





## Appendix C

### Modifications to NLGYRO.ALT for Use With MSC/NASTRAN Version 68

Much of the DMAP language was changed between MSC/NASTRAN Version 68 and earlier versions. Because of this change, two minor changes in the original version 66b NLGYRO.ALT DMAP source code (obtained from MSC) are required for it to execute properly under MSC/NASTRAN version 68. These modifications follow.

1. In line 1 (ignoring comments), change

```
ALTER 492 $
```

to

```
ALTER 504 $
```

2. In line 23, change

```
VECPLOT      , ,BGPDT,EQEXIN,CSTM, , ,/RBGLOBAL///4/ $
```

to

```
VECPLOT      , ,BGPDT,EQEXIN,CSTM, , , ,/RBGLOBAL///4/ $
```

(i.e., add two commas after CSTM.)



## References

1. Anon.: *MSC/NASTRAN User's Manual—MSC/NASTRAN Version 66*. MacNeal-Schwendler Corp., 1988.
2. Joseph, Jerrard A., ed.: *MSC/NASTRAN Application Manual—MSC/NASTRAN Version 66A*. MacNeal-Schwendler Corp., 1991.
3. Mack, Wayne V., ed.: *MSC/DYNA Theoretical Manual—MSC/DYNA Version 1*. MacNeal-Schwendler Corp., 1989.
4. Lee, Sang H., ed.: *Preliminary MSC/NASTRAN Handbook for Nonlinear Analysis*. MacNeal-Schwendler Corp., 1991.
5. Lawrence, Charles; Aiello, Robert A.; Ernst, Michael A.; and McGee, Oliver G.: *A NASTRAN Primer for the Analysis of Rotating Flexible Blades*. NASA TM-89861, 1987.
6. McGee, Oliver G.: *Finite Element Analysis of Flexible, Rotating Blades*. NASA TM-89906, 1987.





